

## A NEW METHOD TO MEASURE THE SPATIAL ARC RESISTANCE DISTRIBUTION OF AN AXIAL BLOWN SWITCHING ARC

M. Hoffacker<sup>1\*</sup>, J. Knauel<sup>2</sup>, P.G. Nikolic<sup>3</sup>, A. Kurz<sup>4</sup> and A. Schnettler<sup>5</sup>

<sup>1-5</sup> Institute for High Voltage Technology, RWTH-Aachen University, Schinkelstr. 2, 52056 Aachen, Germany

\*Email: hoffacker@ifht.rwth-aachen.de

**Abstract:** Since many years the development of gas circuit breakers is surrounded by computational fluid dynamics simulations. The physical models of these simulations are often crosschecked by experiments. One of the aspects related to the interruption capability of the circuit breaker is the spatial arc resistance distribution of the arc. However, it could not yet be determined by experiments as all known methods have either an influence on the arc and the gas flow or can only be applied at special conditions. The aim of the ongoing research project is the development of a new method to determine the spatial arc resistance distribution of a quenched switching arc.

### 1 INTRODUCTION

Circuit breakers are important elements of the electric power supply system. They are required for the safe switching of rated and short-circuit currents. Today's high voltage power supply system's make use of self blast circuit breakers filled with sulphur hexafluoride (SF<sub>6</sub>) as insulating and quenching gas, predominantly. Due to the contact separation during the switch-off process an electric arc is formed between the contacts. By cooling with a forced flow of the quenching gas along the axis of the arc the energy is withdrawn until the arc is extinguished. This cooling process leads to an increasing arc resistance. The value of the resistance and its spatial distribution along the arc are crucial factors for the switch-off process to be successful [1].

The resistance of a switching arc at current zero is mainly influenced by the convective and turbulent cooling of the quenching gas flow [2]. The convective cooling dominates at the stagnation point, the turbulent cooling in the outer nozzle areas. This leads to a non-linear arc resistance distribution near current zero [3].

Research and development projects related to circuit breakers deal more and more with computational fluid dynamics (CFD) simulations. These simulations can replace expensive experiments and allow the visualization of physical values which are not – or only very difficult – accessible in experimental investigations. Thus, they can also improve the understanding of the physical processes in the plasma of the electric arc during the switching operation of a self blast circuit breaker. Therefore the implemented simulation models must be verified on the basis of adequate experiments.

The spatial arc resistance distribution along the axis of the arc is a physical value which is very difficult to determine in experiments and has not yet been in the scope of international research. By

measuring the spatial arc resistance distribution of an axial blown arc at different flow conditions the physical models for simulations can be verified and improved. Therefore it is of high importance that the arc and the gas flow are not influenced by the measurement.

A new method for the indirect measurement of the spatial arc resistance distribution has been developed at the Institute for High Voltage Technology at RWTH Aachen University. This method is based on the detection of the electric field caused by the arc by means of capacitive sensors and is introduced in this paper.

### 2 APPROACH

#### 2.1 Measurement principle

First, the measurement of the spatial arc resistance distribution has to be non invasive. Second an optical access is not possible as the axial blown arc is surrounded by a nozzle, which is typically made of polytetrafluorethylene (PTFE). Due to this the electric field surrounding the arcing zone is used to determine the spatial arc resistance distribution:

**Capacitive field probes:** For the measurement of the spatial arc resistance distribution the potential drop along the axis of the arc is determined. The arc resistance distribution is then calculated by knowing the current. Therefore a reference potential is required which is created by mounting a conductive shield around the insulation nozzle. The cylinder is then connected to ground. Measuring electrodes are placed between this cylinder and the nozzle (figure 1) to measure the arc potential. The material of the nozzle acts as a dielectric and separates the measuring electrode from the arc. This construction is a capacitive field probe [4]. Between electrode and grounded cladding tube a capacity  $C_e$  is generated.

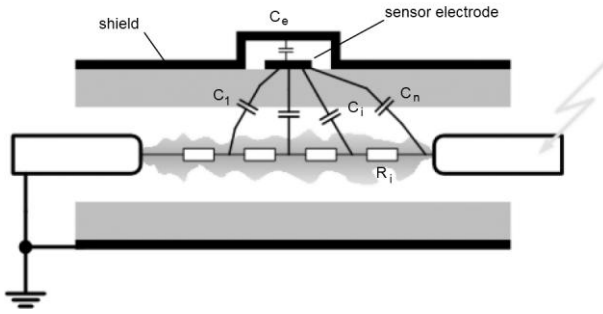


**Figure 1:** Measuring principle (sketch).

Furthermore this construction yields to different stray capacitances  $C_i$  between arc and measuring electrode. The sum of all these capacitances  $C_1 \dots C_n$  is the coupling capacitance between the sensor and the arc. This setup corresponds to a capacitive divider with  $C_i$  as the upper capacitance of the divider and  $C_e$  as lower capacitance of the divider. For measuring the potential distribution several sensors are located along the axis of the arc. Each sensor is measuring a partial voltage of the arc.

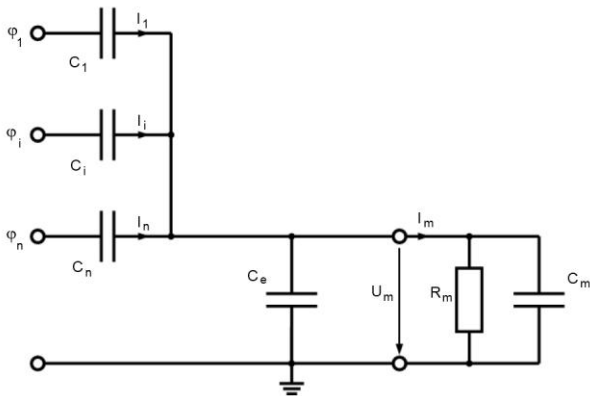


**Figure 2:** Model of capacitive coupling on one sensor including the input impedance of the measurement electronic as ohmic-capacitive load

In figure 2 a model of the signal-coupling of one exemplary sensor loaded with  $R_m$  and  $C_m$  is given. With given arc potentials  $\varphi_i$  the measured voltage at the sensor electrode is calculated by:

$$U_m = \frac{\sum_{i=1}^n C_i \varphi_i}{C_m + \sum_{i=1}^n C_i - \frac{j}{R_m \omega}} \quad (1)$$

By knowing the signal of multiple sensors, the coupling capacitances  $C_i$  and the current the spatial arc resistance distribution can be calculated. Therefore the potential of the arc in front of the sensor should have the highest influence on the measured voltage. Thus the coupling capacitance  $C_i$  which is lineal from sensor to arc should have a high value while the

capacitances beside should have low values. This can be established by design features. To achieve a linear frequency response of the transfer function of the system the load resistance  $R_m$  has to be as high as possible with respect to the band width of the signal to be measured.

**Arc radius and position:** The position and radius of an axially blown switching arc change with time. Thus the coupling capacitances will change with time and position as well. First it is shown that the influence of the radius of the arc can be determined by two sensors at the same part of the arc:

Assuming axial symmetry and the fact that a short part of the arc with the length  $\Delta x_i$  is an ideal cylindrical conductor with the radius  $r_{arc}$  the measured sensor voltage  $U_m'$  can be calculated by setting  $n = 1$  in formula 1:

$$U_m' = \frac{C_i' \varphi_i}{C_m + C_i' - \frac{j}{R_m \omega}} \quad (2)$$

The coupling capacity  $C_i'$  between the measuring electrode and the short part of the arc consists of the capacitance of the nozzle material – which is constant – and the capacitance between arc and nozzle – which depends on the arc radius – in series. Thus the coupling capacity can be calculated:

$$C_i' = C_{i,iso} \left\| \left\| 2\pi \varepsilon_0 \varepsilon_r \frac{\Delta x}{\ln\left(\frac{r_{nozzle}}{r_{arc}}\right)} \right. \right. \quad (3)$$

where

$$C_1 \left\| C_2 = \frac{C_1 \cdot C_2}{C_1 + C_2} \quad (4)$$

As long as the capacitances respectively the nozzle radius are known the measured sensor voltage  $U'$  is only dependent on the arc potential  $\varphi_i$  and the radius  $r_{arc}$  of the arc.

For being able to solve the unknown variables,  $\varphi_i$  and  $r_{arc}$ , a second measuring electrode is placed at the same short part of the arc using a different coupling capacitance. Analogue to formulas 2 and 3 the measured voltage  $U_m''$  can be calculated:

$$U_m'' = \frac{C_i'' \varphi_i}{C_m + C_i'' - \frac{j}{R_m \omega}} \quad (5)$$

$$C_i'' = C_{i,iso}'' \left\| \left\| 2\pi\epsilon_0\epsilon_r \frac{\Delta x}{\ln\left(\frac{r_{nozzle}}{r_{arc}}\right)} \right. \right. \quad (6)$$

Thus both unknown variables ( $\varphi_i$  and  $r_{arc}$ ) can now be determined by these two equations.

However the assumed symmetry along the rotational axis will not occur in the experiment. The arc will move inside the insulation nozzle. Hence the assumption of a cylinder symmetric arrangement is not valid. To be able to determine position, thickness and potential of the arc anyway the amount of field probes is increased. By placing four sensors surrounding the same short part of the arc the system of equations can be solved.

## 2.2 Test Setup

**Test device:** For the measurement of the spatial arc resistance distribution of an axially blown switching arc a test device is designed. A cross section is shown in figure 3.

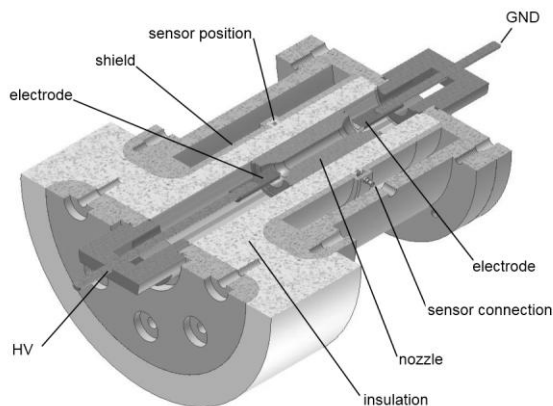


**Figure 3:** Cross section of the test device without blow gas supply.

The modular design allows a change of the inner nozzle and thus the testing of different nozzle geometries. The distance between the arcing electrodes can be adjusted as well. The arc is blown with a gas flow generated by cold, compressed gas from a pressure vessel. Hence the blow gas conditions can be better controlled than by using the self blast effect.

The test object is designed in order to withstand the mechanical forces created by the blowing gas and the arc. Additionally the insulation can withstand the high field stresses generated by the transient recovery voltage (TRV) which can occur in the experiments.

**Capacitive sensors:** In a first approach four capacitive coupled measuring electrodes are placed around an arc burning inside the insulation nozzle. The design is shown in figure 4. Three sensors are identical and separated by an angle of  $120^\circ$  from each other (S1-S3). The fourth sensor (S4) is shifted outwards to achieve a different coupling capacitance.

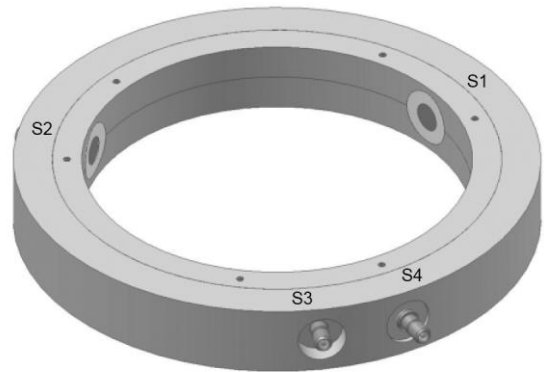


**Figure 4:** Sensor arrangement for the sensors S1-S3 each shifted by  $120^\circ$  and the recessed sensor S4.

As mentioned above the load resistance of the measuring electrode,  $R_m$ , should be as high as possible as the interaction of the coupling capacities  $C_i$ , the stray capacitance  $C_e$  and the capacity of the connecting cable  $C_{cable}$  with the input impedance of the electronic measurement circuit behaves like a low pass filter. A typical measured arcing voltage is transferred into the frequency domain for evaluating the minimum cut off frequency leading to an acceptable error in the measured signal. Figure 5 shows the frequency spectrum of the measured signal (black) and the signal filtered with an ideal low pass filter with  $f_{cut} = 1$  MHz. The original and filtered signals in the time domain are given in figure 6. Here the period around current zero is shown. It can be derived that for this case the error caused by the low pass filter is in the range of 5 % at a point in time 200 ns before current zero. This is also confirmed by applying the theorem of Parseval [5] on the areas below the amplitude for  $0\text{Hz} < f < 1\text{MHz}$  and  $1\text{MHz} < f < 10\text{MHz}$ . For cut off frequencies above 1 MHz the load resistance has to be  $R_m > 10^9 \Omega$ . This can only be achieved by an operational amplifier. In addition this amplifier needs a high bandwidth, a high gain-bandwidth-product (GBWP) and must be stable. These requirements can be fulfilled by some FET-operational amplifiers. But still the output voltage of this amplifier is only in the range of some 100 mV and in the most interesting period (around current zero) even below.

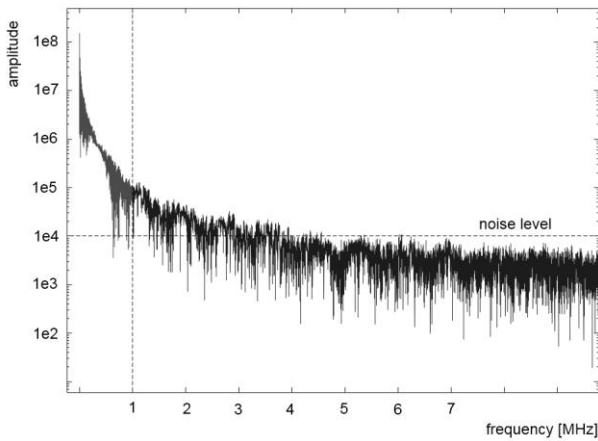


**Figure 5:** Frequency spectrum of a typical arcing voltage caused by the 950 Hz injection current of the test circuit.

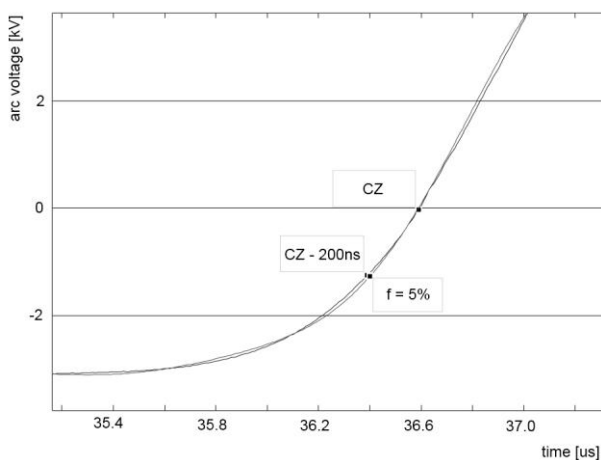


**Figure 6:** Error in the arcing voltage at current zero caused by an ideal low pass with  $f_{\text{cut}} = 1$  MHz.

Due to these disadvantages it is decided not to choose a high resistance  $R_m$  but a very low resistance  $R_m$ . Therefore the capacitance  $C_e$  in figure 2 is almost bypassed by a short circuit. The circuit does not longer behave like a capacitive divider but measures the dielectric current. Thus the measured voltage is proportional to the derivation of the potential  $\varphi_i$ . The equivalent circuit diagram for this differentiating operational amplifier is given in figure 7.

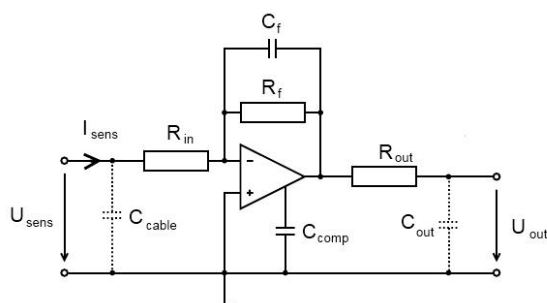


**Figure 7:** Equivalent circuit diagram of the differentiating operational amplifier.

Using a well chosen amplifier, an elaborate design of the circuit board and a compensating capacitance  $C_{\text{comp}}$  a linear increase of the transfer-function with 20 dB / decade up to 10 MHz can be achieved.

**Test circuit:** For igniting and feeding the arc the high voltage part of a synthetic test circuit is used. This is the part of the circuit which is on the right hand side of the device under test (DUT) in figure 8. The capacitance  $C_{\text{HV}}$  is charged to some 10 kV and the ignition spark gap (ISG) is triggered. A resonance circuit with  $f = 950$  Hz is formed by  $C_{\text{HV}}$  and  $L_{\text{HV}}$ . The arc inside the test device is ignited by a thin wire which evaporates due to the high current. The metal vapour from the wire is blown out of the arcing zone within the first half cycle of the resonance circuit. If the test device is able to interrupt this oscillating current at current zero the arcing zone is stressed by the transient recovery voltage which is formed by the elements  $R_p$  and  $C_p$ .

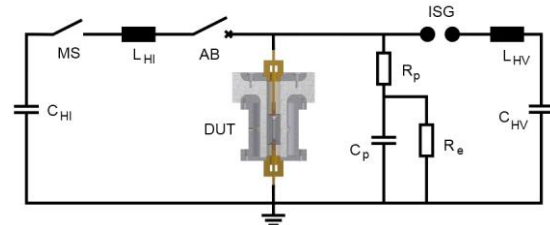


**Figure 8:** Schematic of the used synthetic test circuit.

### 3 RESULTS

For testing the principle feasibility of the developed measuring method, the behaviour of the measuring electrodes, the electric amplifier and the test device basic experiments in the synthetic test circuit are carried out. Here the arc is axially blown with air at ambient temperature from a pressure reservoir.

Before carrying out the arcing experiments the transfer function from the high voltage arcing electrode to each sensor is estimated. While measuring not only the voltages from the sensor electrodes, but also the total arcing voltage, the influence of the arcing electrode on each sensor can be subtracted from the measured signals. Thereafter the signals are integrated.

First the arc is blown non-symmetrically. The gas flow forces the arc to move to the nozzle surface next to sensor S2. The measured total arcing voltages as well as the integrated signals from the measurement electrodes (without influence of the arcing electrode) for this experiment are shown in figure 9. Here the sensor positions according to figure 4 are used. The small distance between the arc and sensor S2 results in a higher capacitance and thus in a higher measurement signal. This behaviour can be observed in an analogue way

when the arc is forced towards sensor S1 and S3, respectively.

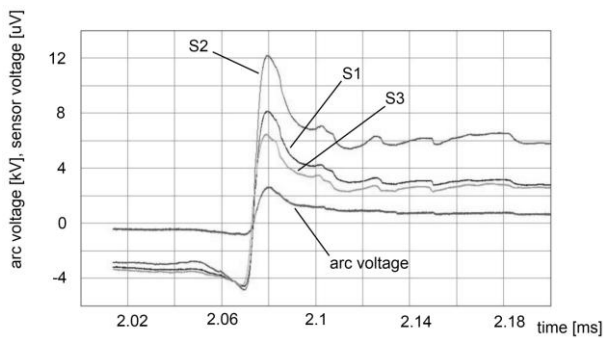


**Figure 9:** Total arcing voltage and integrated sensor voltages of a non-symmetrically blown arc at a fixed position.

The “ripple” in the signals can be found in the total arcing voltage as well. That is a strong indication for an effect of the arcing behaviour and not for a measurement error.

Second the arc is blown symmetrically. Figure 10 shows the signals of 8 sensors distributed along the axis of the arc. Here the arc radius and position are not considered but again the signals are reduced by the influence of the arcing electrode, integrated and scaled. The height of the amplitudes corresponds with the sensor position. The non-linear distance between the signals over time indicates a non-linear arc resistance distribution.

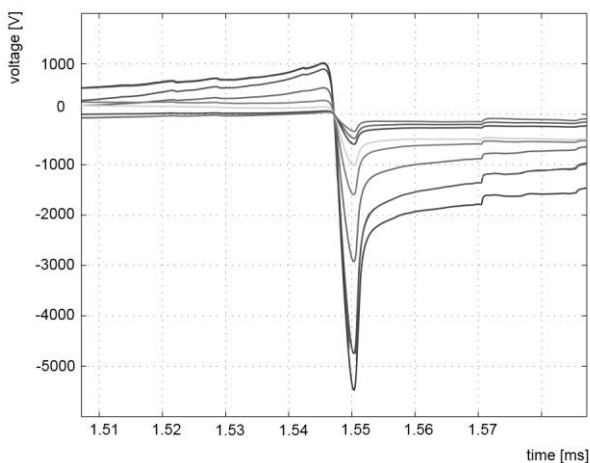


**Figure 10:** Scaled and integrated sensor voltages of a symmetrically blown arc along the arcing axis.

#### 4 SUMMARY AND OUTLOOK

The spatial arc resistance distribution of a blown switching arc is a physical value which could not yet be determined in experiments without influencing the arc. The new method introduced in this paper can be used for fulfilling this task. Therefore capacitive field sensors are used.

First experiments show the feasibility of the new method: The measurement signals indicate the possibility to determine the arc position as well as a potential respectively a resistance distribution.

As the principle feasibility of the method can be shown the next step is placing multiple groups - each consisting of four sensors - along the axis of the arc. For analysing the experimentally measured data a software-tool is developed to calculate the spatial resistance distribution. Here the influence of the arc radius will be considered as well. Therefore the mathematic theory of inverse problems is used.

#### 5 ACKNOWLEDGEMENT

The authors are grateful to M. Koch and T. Wild for their investigations during their studies at RWTH-University.

This project is funded by Deutsche Forschungsgemeinschaft (DFG).

#### 6 REFERENCES

- [1] H. Knobloch, U. Habedank: “Behaviour of SF6 high-voltage circuit breakers with different arc-extinguishing systems at shortline fault switching”; Science, Measurement and Technology; IEE Proceedings; Bd. 148 p273-279, 2001
- [2] C. Franck, P. Skarby, M. Seeger, “Influence of the nozzle geometry on the thermal interruption performance in high-voltage circuit breakers”, Proceedings on the XVI<sup>th</sup> symposium on physics of switching arc, 2005
- [3] M.C. Tang: „Widerstandsverteilung in Schaltlichtbögen von Selbstblasleistungsschaltern während der Stromnulldurchgangsphase“, PHD-thesis, Institute for High Voltage Technology, RWTH-Aachen University, 2010
- [4] A. Küchler: „Erfassung transientser elektromagnetischer Feldverteilungen mit konzentrierten und räumlich ausgedehnten Sensoren“, Fortschritt-Berichte VDI, Reihe 21: 7, Düsseldorf, 1986
- [5] J.-R. Ohm, H. D. Lüke, „Signalübertragung: Grundlagen der digitalen und analogen Nachrichtenübertragungssysteme“, Springer-Verlag, 2010